Journal of Superconductivity and Novel Magnetism (2019) 32:3315–3320
https://doi.org/10.1007/s10948-019-5090-8

ORIGINAL PAPER

Synthesis of the Orthorhombic $Dy_{1-x}Ho_xMnO_3$ Single Crystals and Study of Their Magnetic Properties

S. V. Semenov[1,2] · M. I. Kolkov[1] · K. Yu Terent'ev[1] · N. S. Pavlovskiy[1,2] · M. S. Pavlovskiy[1,2] · A. D. Vasiliev[1,2] · A. V. Shabanov[1] · K. A. Shaykhutdinov[1] · D. A. Balaev[1,2]

Received: 11 January 2019 / Accepted: 25 March 2019 / Published online: 17 April 2019

Abstract
In this report, we prepared for the first time the orthorhombic $Dy_{1-x}Ho_xMnO_3$ single crystals with $x = 0$, 0.1, 0.2, 0.3, and 0.4 using the flux technique. The post-growth processing and chemical and structural characterization of the synthesized samples were performed. Also, we examined the samples obtained by their magnetic properties and the magnetic anisotropy in wide ranges of temperatures and magnetic fields.

Keywords Rare earth manganites · Orthorhombic $Dy_{1-x}Ho_xMnO_3$ · Crystal growth · Magnetic anisotropy

1 Introduction

In recent years, rare earth manganites $RMnO_3$ (R is a rare earth ion) belonging to the class of multiferroic materials have been intensively investigated [1–19]. The strong interrelation between the electrical and magnetic properties of these compounds gives rise to a wide diversity of intriguing phenomena [1–8] and makes these materials promising for application [1]. It is well-known that the $RMnO_3$ crystal structure is determined by the radius of a rare earth ion. In particular, using a conventional solid-state synthesis technique under normal conditions, one can obtain the $RMnO_3$ compounds with either the orthorhombic (R = La….Dy) or hexagonal (R = Ho….Lu, Y, Sc) structure [2]. In addition, using different synthesis techniques or changing the environmental conditions (gas environment, temperature, or pressure), one can obtain the $RMnO_3$ compounds of different structural modifications [2–6]. The authors of studies [3, 4] used optical zone melt to synthesize $DyMnO_3$ single crystals with the orthorhombic (air) and hexagonal (argon atmosphere) modification. The $RMnO_3$ compound containing the rare earth elements (R = Ho….Lu) with a smaller ionic radius as compared with Dy one, which usually have the hexagonal structure, can also be obtained in the orthorhombic modification using, e.g., high-temperature synthesis [2] or the flux method [5]. On the contrary, hexagonal single crystals with larger-radius rare earth elements (La….Tb) are fairly difficult to obtain. However, the transition from the orthorhombic to hexagonal phase can be implemented, as was made in [6] for the $Tb_{1-x}Y_xMnO_3$ system using partial replacement of large rare earth ions by ions with a smaller radius.

In addition, the physical (magnetic and dielectric) properties of the $RMnO_3$ system depend on the type of a rare earth ion. In particular, the hexagonal $RMnO_3$ compounds are characterized by the high temperature (800–900 K) of the intrinsic ferroelectric transition [7] and a complex magnetic phase diagram [8, 9]. For instance, the $HoMnO_3$ compound undergoes three magnetic phase transitions with a decrease in temperature, specifically, (i) antiferromagnetic ordering of Mn^{3+} ions at $T_N \sim 75$ K, (ii) spin-reorientation transition at temperatures of $T = 30$–35 K, and (iii) antiferromagnetic ordering of the rare earth subsystem around $T = 4$–5 K [10].

In contrast to the hexagonal manganites, the orthorhombic rare earth manganites represent improper ferroelectrics, which are spontaneously polarized upon variation in the magnetic structure [11–14]. The temperature evolution of the magnetic structure of the orthorhombic $RMnO_3$ compounds was examined in studies [15–17]. It was found that at T_N (38, 39, and 41 K for R = Ho, Dy, and Tb, respectively), the incommensurate antiferromagnetic order is established, which represents a

✉ S. V. Semenov
svsemenov@iph.krasn.ru

[1] Kirensky Institute of Physics, Federal Research Center KSC SB RAS, Krasnoyarsk 660036, Russia

[2] Siberian Federal University, Krasnoyarsk 660041, Russia

Table 1 $Dy_{1-x}Ho_xMnO_3$ solid solution furnace charge composition

	PbO, g	PbF_2, g	B_2O_3, g	MnO_2, g	Dy_2O_3, g	Ho_2O_3, g
$DyMnO_3$	157.74	29.586	0.3	6.63	14.22	–
$Dy_{0,9}Ho_{0,1}MnO_3$	157.74	29.586	0.3	7.904	15.252	1.718
$Dy_{0,8}Ho_{0,2}MnO_3$	190.9749	33.14638	0.4	7.903636	13.56364	3.435091
$Dy_{0,7}Ho_{0,3}MnO_3$	159.56	29.927	0.3	6.688	10.04	4.36
$Dy_{0,6}Ho_{0,4}MnO_3$	159.72	29.958	0.3	6.688	8.608	5.813

sinusoidally modulated collinear structure consisting of only manganese magnetic moments. With a further decrease in temperature, at $T \sim 18–20$ K, the transition to the noncentrosymmetric spiral magnetic structure occurs due to the competition (frustration) of the exchange couplings; in this case, the magnetic moments of a rare earth element, similar to the manganese ones, are aligned helically. The absence of an inversion center and the nonuniform magnetoelectric interaction lead to the occurrence of the electric polarization [7]. The spontaneous polarization is observed below the temperature of the ferroelectric transition (20–30 K) until the rare earth subsystem ordering temperature (4–7 K), at which the spiral magnetic structure is collapsed [11, 18, 19].

The temperature region of existence of the spontaneous polarization can be broadened by partial substitution in the rare earth subsystem, as was made in [18, 19], where the magnetic and ferroelectric properties of the polycrystalline $Dy_{1-x}Ho_xMnO_3$ solid solutions were investigated in a wide concentration range. It was found that partial substitution of Ho ions for Dy ions strongly suppresses the independent spin order of Dy ions at low temperatures and maintains the strong R–Mn spin coupling, which noticeably enhances the polarization at low temperatures [18]. In addition, Zhang et al. [19] reported a detailed phase diagram for the $Dy_{1-x}Ho_xMnO_3$ system over the entire substitute concentration range (from $x = 0$ to $x = 1$). However, in the above-cited works, the experiments were conducted on polycrystalline samples, which did not allow the anisotropy of the magnetic and magnetoelectric properties to be investigated.

Thus, the synthesis of high-quality single-phase $Dy_{1-x}Ho_xMnO_3$ single crystals and study of their magnetic properties is of great practical importance.

2 Experimental

To obtain $Dy_{1-x}Ho_xMnO_3$ single crystals, we chose spontaneous crystallization from the flux. The $Dy_{1-x}Ho_xMnO_3$ single crystals with substitute concentrations of $x = 0$, 0.1, 0.2, 0.3, and 0.4 were successfully synthesized. At the higher holmium concentrations, the synthesis failed; thus, we established the limit holmium concentration in the $Dy_{1-x}Ho_xMnO_3$ system.

Since the $Dy_{1-x}Ho_xMnO_3$ melting points stay within the possibility of available muffle furnaces, the high-efficiency sintering was ensured by adding the stoichiometric mixture of the initial MnO_2, Dy_2O_3, and Ho_2O_3 oxides with a solvent in a ratio of 9:1.

Table 1 gives data on the furnace charge of the prepared $Dy_{1-x}Ho_xMnO_3$ solid solutions. As a solvent, we used an available PbO–PbF_2–B_2O_3 system with a low melting point and high solvent strength. The melting points for all the compositions were determined upon slow heating for 12 h. They ranged from 750 to 1100 °C. After that, a 2-week-long synthesis was performed for each composition with a substitute concentration step of 0.1. The procedure included smooth heating to a temperature of 1200 °C for 12 h, 1-day exposure, and slow cooling to 750 °C at a rate of 2.3 °C/h. The $Dy_{1-x}Ho_xMnO_3$ single crystals with $x = 0–0.4$ and with the average size $1 \times 1 \times 1.5$ mm^3 were obtained. An example of a typical obtained single crystal is shown in Fig. 1. The direction of the crystallographic axes was determined by the shape of the samples, as shown in Fig.1.

The crystal structure of the synthesized samples was studied by X-ray powder diffraction on a BRUKER D8 ADVANCE diffractometer at room temperature.

Figure 2 shows X-ray powder diffraction patterns of the synthesized samples. An analysis of the $Dy_{1-x}Ho_xMnO_3$ ($x = 0–0.4$) samples showed that the prepared

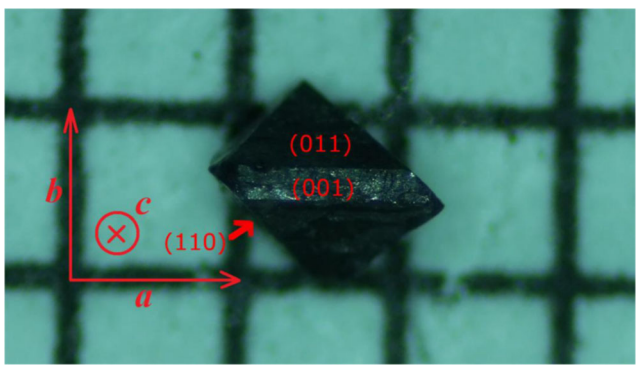

Fig. 1 Single crystal of $Dy_{0,8}Ho_{0,2}MnO_3$

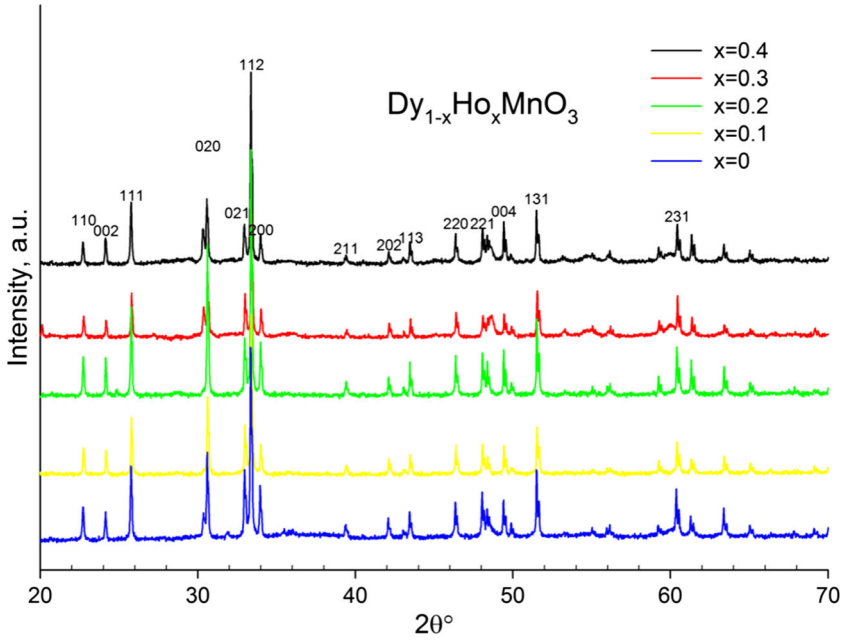

Fig. 2 X-ray powder diffraction pattern of the synthesized single crystals

compounds are orthorhombic (sp. gr. *Pbnm*) and, in addition to, there are no reflections of the hexagonal modification. The lattice parameters and unit cell volumes for all the samples are given in Table 2. It can be seen that with an increase in the x value, the unit cell volume decreases, which is quite obvious, since the holmium ion is smaller than dysprosium one. Studies carried out on a single-crystal X-ray diffractometer (not shown in the article) confirmed the high quality of the samples.

The chemical composition of the samples was studied by energy-dispersive X-ray spectroscopy (EDS) on a Hitachi-TM 3000 electron microscope. According to the EDS data, the chemical composition of the samples is similar to nominal. The EDS data for all the samples are given in Table 3.

Thus, we synthesized for the first time the $Dy_{1-x}Ho_xMnO_3$ ($x = 0$, 0.1, 0.2, 0.3, and 0.4) manganite single crystals of the orthorhombic modification by spontaneous crystallization from the flux. The synthesized samples were subjected to the post-growth processing and chemical and structural characterization.

Table 2 Lattice parameters and unit cell volumes of the $Dy_{1-x}Ho_xMnO_3$ compound

$Dy_{1-x}Ho_xMnO_3$	a, Å	b, Å	c, Å	V, Å^3
$x = 0$	5.2816	5.8457	7.3802	227.8610
$x = 0.1$	5.2787	5.8446	7.3772	227.5984
$x = 0.2$	5.2768	5.8432	7.3759	227.4233
$x = 0.3$	5.2748	5.8432	7.3730	227.2504
$x = 0.4$	5.2721	5.8449	7.3716	227.1522

3 Study of the Magnetic Properties

The magnetic properties of the obtained single-crystal samples were experimentally investigated in wide temperature and magnetic field ranges. The magnetic anisotropy of the samples was examined.

The magnetic parameters of the $Ho_{1-x}Dy_xMnO_3$ single crystals were measured on a vibrating sample magnetometer with a superconducting solenoid [20], which allows the magnetization to be measured in the temperature range of 4.2–300 K in applied magnetic fields of up to 8 T.

Figure 3 shows temperature dependences of magnetization for all the samples measured in the zero-field cooling (ZFC) conditions in an external magnetic field of $H = 1$ kOe applied along different crystallographic directions.

It can be seen in Fig. 3 that the investigated single crystals are characterized by a significant magnetic anisotropy. In addition, the M(T) dependences measured along the a and b axes for all the samples have a maximum corresponding to the temperature T_N of antiferromagnetic ordering of the rare earth subsystem. The concentration dependence of the ordering temperature is presented in

Table 3 Energy-dispersive X-ray spectroscopy data for all the samples

$Dy_{1-x}Ho_xMnO_3$	$x = 0$	$x = 0.1$	$x = 0.2$	$x = 0.3$	$x = 0.4$
Dy, mass. % (norm.)	54.90	48.20	41.22	38.54	32.55
Ho, mass. % (norm.)	0%	5.27	10.27	16.48	21.30
Dy/Ho, (expected)		8.87	3.94	2.3	1.47
Dy/Ho (EDS)		9.15	4.01	2.34	1.53

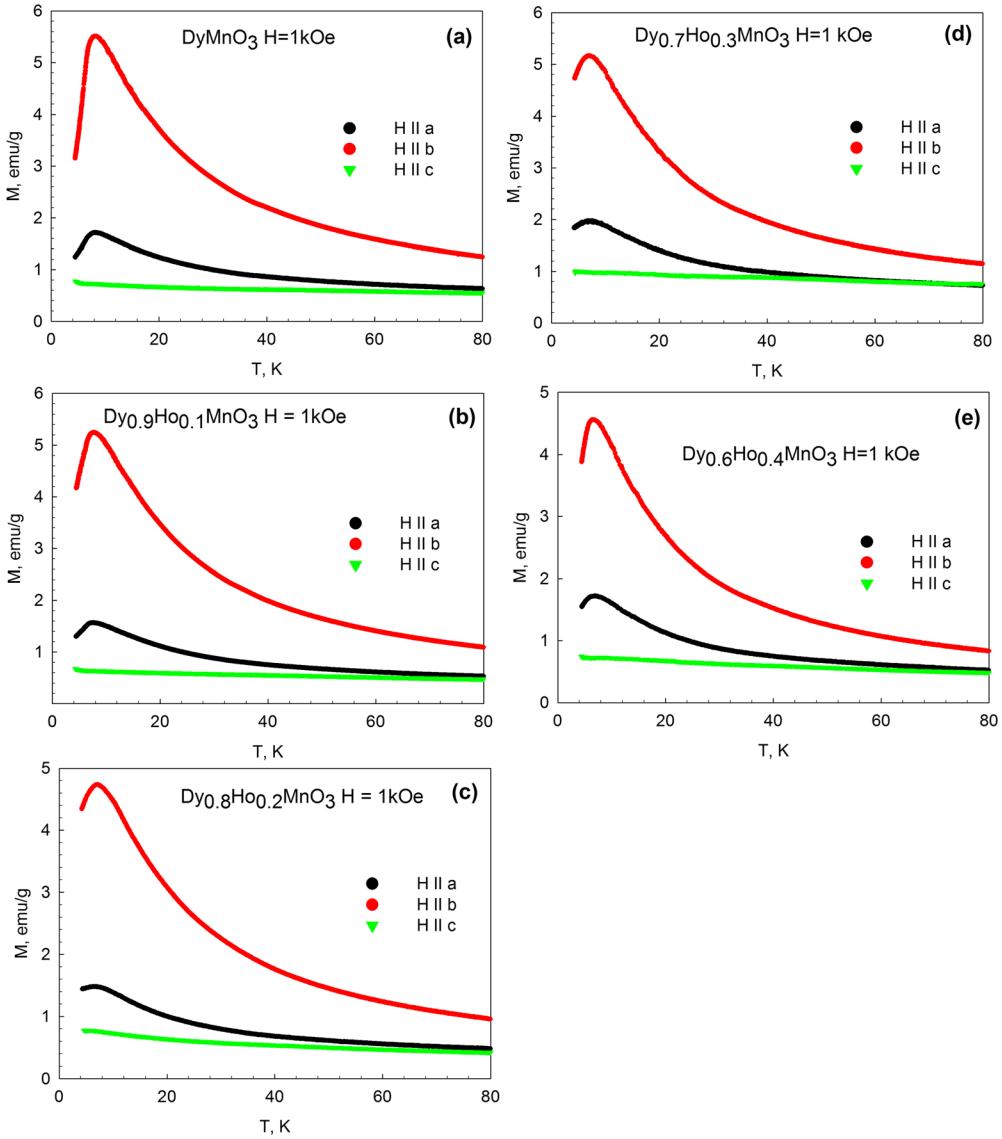

Fig. 3 Temperature dependences of magnetization for the $Dy_{1-x}Ho_xMnO_3$ single crystals with $x =$ **a** 0, **b** 0.1, **c** 0.2, **d** 0.3, and **e** 0.4 measured in a magnetic field $H = 1$ kOe applied in different crystallographic directions

Fig. 4. It can be seen that with an increase in the Ho concentration, the Neel temperature monotonically decreases. No pronounced anomalies around $T \sim 40$ K, which correspond to the antiferromagnetic ordering of Mn magnetic moments, are observed in temperature dependences of magnetization measured along the *c* axes.

Figure 5 shows field dependences of magnetization measured in different crystallographic directions at $T = 4.2$ K. For all the synthesized samples, one can observe a significant anisotropy of the magnetic properties; the magnetization along the *b* axis is approximately twice as high as that along the *a* axis and exceeds the anisotropy along the *c* axis by a factor of six. In addition, it can be seen that the M(H) dependences measured along the *a* and *b* axes are nonmonotonic.

For comparison, Fig. 6 shows field dependences of the magnetic moment in Bohr magnetons μ_B recalculated per a

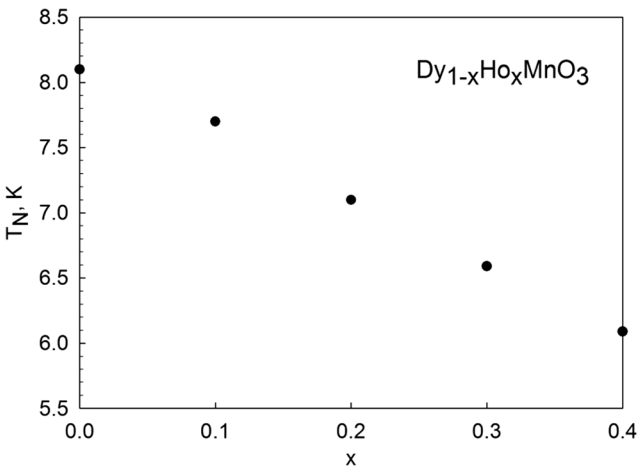

Fig. 4 Concentration dependences of temperature T_N of the ordering of the $Dy_{1-x}Ho_xMnO_3$ rare earth subsystem

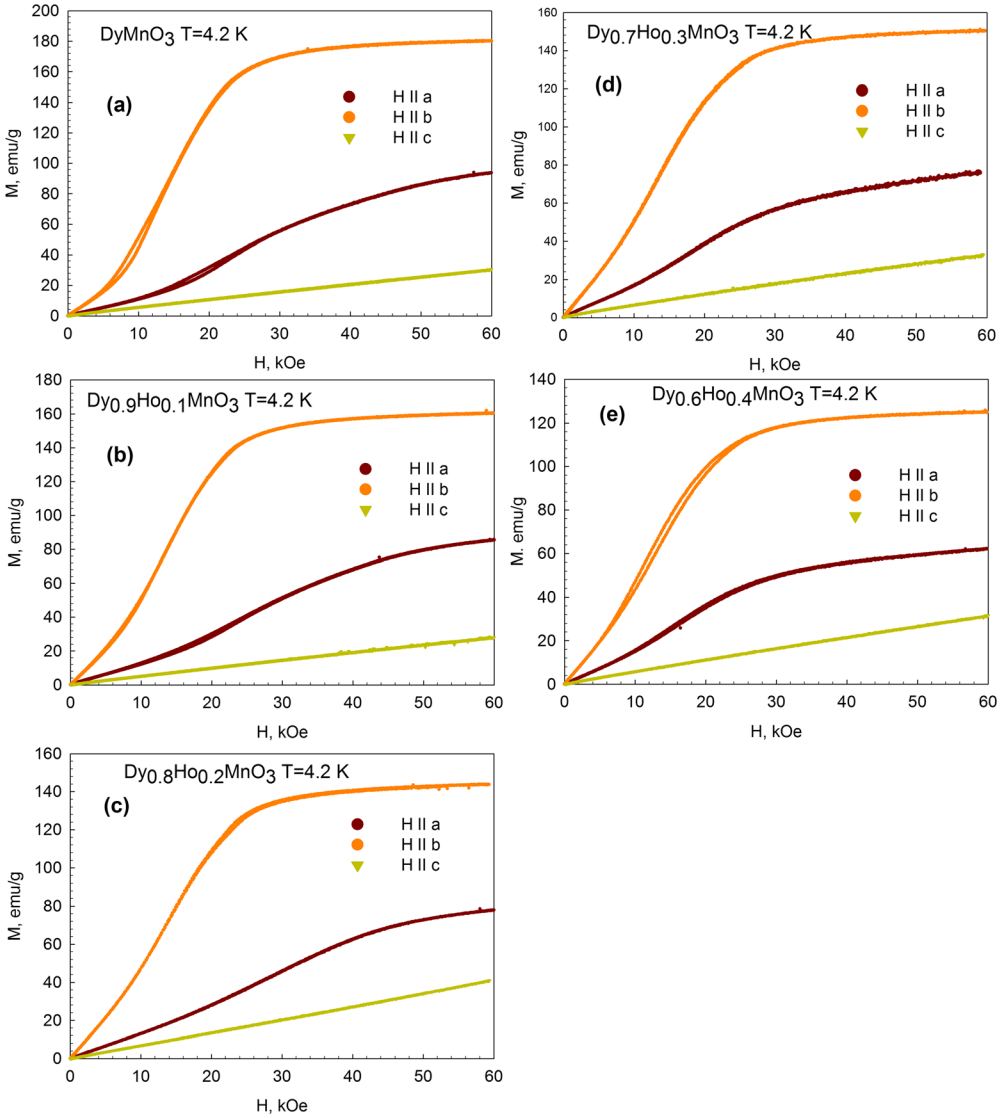

Fig. 5 Field dependences of magnetization for the $Dy_{1-x}Ho_xMnO_3$ single crystals with $x =$ **a** 0, **b** 0.1, **c** 0.2, **d** 0.3, and **e** 0.4 measured in magnetic fields applied in different crystallographic directions at $T = 4.2$ K

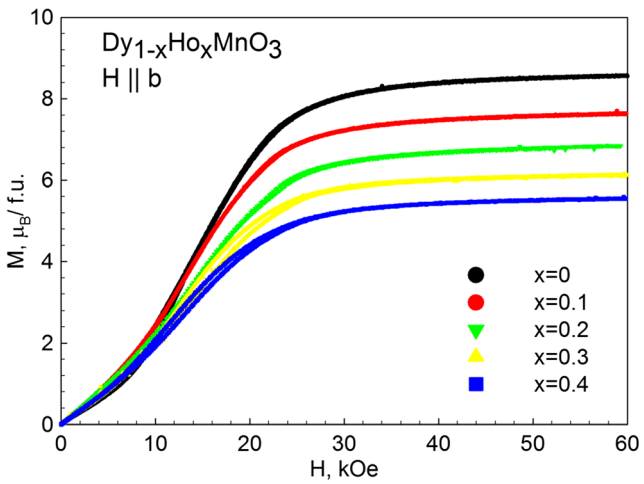

Fig. 6 Field dependences of magnetization for the $Dy_{1-x}Ho_xMnO_3$ single crystals measured along the *b* axis

$Dy_{1-x}Ho_xMnO_3$ formula unit for all the samples measured along the *b* axis at $T = 4.2$ K. It can be seen that the magnetic moment monotonically decreases with an increase in the Ho concentration.

4 Conclusion

Thus, we obtained the following results:

- The orthorhombic $Dy_{1-x}Ho_xMnO_3$ manganite single crystals with $x = 0$, 0.1, 0.2, 0.3, and 0.4 were obtained for the first time by spontaneous crystallization from the flux. The post-growth processing and chemical and structural characterization of the synthesized samples were performed.

- The magnetic properties of the synthesized single-crystal samples were experimentally investigated in wide ranges of temperatures and magnetic fields. The magnetic anisotropy of the synthesized single-crystal samples was examined.

Funding The reported study was funded by Russian Foundation for Basic Research, Government of Krasnoyarsk Territory, Krasnoyarsk Regional Fund of Science to the research project: "Research, synthesis and investigation of new oxide single crystals showing the interrelation of magnetic, magnetoelastic and magnetoelectric properties" (project № 18-42-243024).

References

1. Fiebig, M., Lottermoser, T., Lonkai, T., Goltsev, A.V., Pisarev, R.V.: Magnetoelectric effects in multiferroic manganites. J. Magn. Magn. Mater. **290**, 883–890 (2005)
2. Zhou, J.S., Goodenough, J.B., Gallardo-Amores, J.M., Morán, E., Alario-Franco, M.A., Caudillo, R.: Hexagonal versus perovskite phase of manganite RMnO3 (R = Y, Ho, Er, Tm, Yb, Lu). Phys. Rev. B. **74**, 014422 (2006)
3. Ivanov, V.Y., Mukhin, A.A., Prokhorov, A.S., Balbashov, A.M., Iskhakova, L.D.: Magnetic properties and phase transitions in the DyMnO single crystals. Phys. Solid State. **48**, 1726–1729 (2006)
4. Harikrishnan, S., Rößler, S., Kumar, C.N., Bhat, H.L., Rößler, U.K., Wirth, S., Elizabeth, S.: Phase transitions and rare-earth magnetism in hexagonal and orthoorthorhombic DyMnO3 single crystals. J. Phys.: Condensed Matt. **21**, 096002 (2009)
5. Lee, N., Choi, Y.J., Ramazanoglu, M., Ratcliff, W., I, I., Kiryukhin, V., Cheong, S.W.: Mechanism of exchange striction of ferroelectricity in multiferroic orthoorthorhombic HoMnO 3 single crystals. Phys. Rev. B. **84**, 020101 (2011)
6. Ivanov, V.Y., Mukhin, A.A., Prokhorov, A.S., Balbashov, A.M., Iskhakova, L.D.: Magnetic and dielectric properties of orthoorthorhombic and hexagonal multiferroics in the Tb _1-x Y _x MnO _3 system. JETP Lett. **91**, 424–430 (2010)
7. Smolenskiĭ, G.A., Chupis, I.E.: Ferroelectromagnets. Sov. Phys. Usp. **25**, 475 (1982)
8. Pękała, M., Wolff-Fabris, F., Fagnard, J.F., Vanderbemden, P., Mucha, J., Gospodinov, M.M., Ausloos, M.: Magnetic properties and anisotropy of orthoorthorhombic DyMnO3 single crystal. J. Magn. Magn. Mater. **335**, 46–52 (2013)
9. Dubrovskiy, A.A., Pavlovskiy, N.S., Semenov, S.V., Terent'Ev, K.Y., Shaykhutdinov, K.A.: The magnetostriction of the HoMnO3 hexagonal single crystals. J. Magn. Magn. Mater. **440**, 44–46 (2017)
10. Pavlovskii, N.S., Dubrovskii, A.A., Nikitin, S.E., Semenov, S.V., Terent'ev, K.Y., Shaikhutdinov, K.A.: Magnetostriction of hexagonal HoMnO 3 and YMnO 3 single crystals. Phys. Solid State. **60**, 520–526 (2018)
11. Kimura, T., Goto, T., Shintani, H., Ishizaka, K., Arima, T.H., Tokura, Y.: Magnetic control of ferroelectric polarization. Nature. **426**, 55 (2003)
12. Kimura, T., Lawes, G., Goto, T., Tokura, Y., Ramirez, A.P.: Magnetoelectric phase diagrams of orthoorthorhombic RMnO3 (R = Gd, Tb, and Dy). Phys. Rev. B. **71**, 224425 (2005)
13. Arima, T., Goto, T., Yamasaki, Y., Miyasaka, S., Ishii, K., Tsubota, M., Tokura, Y.: Magnetic-field-induced transition in the lattice modulation of colossal magnetoelectric GdMnO3 and TbMnO3 compounds. Phys. Rev. B. **72**, 100102 (2005)
14. Yamasaki, Y., Sagayama, H., Abe, N., Arima, T., Sasai, K., Matsuura, M., Tokura, Y.: Cycloidal spin order in the a-axis polarized ferroelectric phase of orthoorthorhombic perovskite manganites. Phys. Rev. Lett. **101**, 097204 (2008)
15. Feyerherm, R., Dudzik, E., Aliouane, N., Argyriou, D.N.: Commensurate Dy magnetic ordering associated with incommensurate lattice distortion in multiferroic DyMnO3. Phys. Rev. B. **73**, 180401 (2006)
16. Kenzelmann, M., Harris, A.B., Jonas, S., Broholm, C., Schefer, J., Kim, S.B., Lynn, J.W.: Magnetic inversion symmetry breaking and ferroelectricity in TbMnO3. Phys. Rev. Lett. **95**, 087206 (2005)
17. Schierle, E., Soltwisch, V., Schmitz, D., Feyerherm, R., Maljuk, A., Yokaichiya, F., Weschke, E.: Cycloidal order of 4 f moments as a probe of chiral domains in DyMnO3. Phys. Rev. Lett. **105**, 167207 (2010)
18. Zhang, N., Guo, Y.Y., Lin, L., Dong, S., Yan, Z.B., Li, X.G., Liu, J.M.: Ho substitution suppresses collinear Dy spin order and enhances polarization in DyMnO3. Appl. Phys. Lett. **99**, 102509 (2011)
19. Zhang, N., Dong, S., Fu, Z., Yan, Z., Chang, F., Liu, J.: Phase transition and phase separation in multiferroic orthoorthorhombic Dy 1− x Ho x MnO 3 ($0 \le x \le 1$). Sci. Rep. **4**, 6506 (2014)
20. Balaev, A.D., Boyarshinov, Y.V., Karpenko, M.M., Khrustalev, B.P.: Automated magnetometer with superconducting solenoid. Prib. Tekh. Eksp. **3**, 167 (1985)